



Attentional capacity limit for visual search causes spatial neglect in normal observers

M.J. Morgan, J.A. Solomon *

The Henry Wellcome Laboratories for Vision Sciences, Applied Vision Research Centre, City University, Northampton Square, London EC1V 0HB, UK

Received 10 November 2004; received in revised form 18 November 2005

Abstract

When observers simultaneously monitor several positions in the visual field, distracting stimuli have a devastating effect on the ability to discriminate between similar shapes. For example, the minimum tilt necessary for an observer to discriminate between a clockwise and anticlockwise tilt has been shown to increase with the square root of the number of untilted distractors. Here we show that these rapid visual searches remain inefficient even with extended practice. Moreover, each of our observers performed particularly poorly when uncued targets appeared in certain idiosyncratic positions, as though he or she neglected to process part of the visual field. This type of neglect is not commensurate with the popular ‘max rule’ strategy, in which observers simply report the direction of the largest apparent tilt. Nor is it consistent with tilt averaging. It is, however, consistent with an attentional effect in which both the signal and the noise from neglected positions are decreased, leaving the local signal/noise ratio constant. We show that our data can be well fit by models in which discriminations are based on a combination of these locally weighted, noisy signals.

© 2005 Elsevier Ltd. All rights reserved.

Keywords: Search; Neglect; Orientation

1. Introduction

Visual search experiments have long suggested a role for attention in pattern discrimination, but whether this indicates a capacity limit in low-level vision remains controversial. An alternative explanation is that distractors are noisily encoded, so that they are potentially confusable with the target; the observer reacts to this ambiguity by choosing the noisy stimulus that is least like the distractor prototype (the so-called ‘max rule’). In the popular orientation–identification task (see Fig. 1) (Baldassi & Burr, 2000; Carrasco, Talgar, & Cameron, 2001; Parkes, Lund, Angelucci, Solomon, & Morgan, 2001; Solomon & Morgan, 2001), widely spaced distractors have their greatest effect when displays end with a postmask (Morgan, Castet, & Ward, 1998). On the other hand, with long exposures, and/or no postmask, set-size effects are smaller and

consistent with the Max Rule, described above (for a review see Morgan & Solomon, 2005). Since observers can *locate* the sole tilted target, and therefore use some type of Max Rule in brief, postmasked displays (Solomon & Morgan, 2001), we wondered why they did not use the max rule when asked to identify that target.

Before tackling that paradox, we wanted to assure ourselves that expert observers could not learn to adopt the max rule with sufficient practice. So (author) MM and two other well-trained psychophysical observers, naïve to our purpose, each performed between 1400 and 2800 trials of the orientation–identification task illustrated in Fig. 1. Before we describe the results, we first need to elaborate on our use of the phrase ‘widely spaced,’ above. When the distance between target and distractors is sufficiently small, set-size effects can be very large without postmasks, *even when the observer knows where the target is* (Parkes et al., 2001). Since these ‘crowded’ displays apparently preclude use of the max rule (Palmer, 1994; Palmer, Verghese, & Pavel, 2000), we therefore decided that our target and distractors had to be sufficiently spaced to avoid crowding.

* Corresponding author. Fax: +44 20 7040 0182.

E-mail address: J.A.Solomon@city.ac.uk (J.A. Solomon).

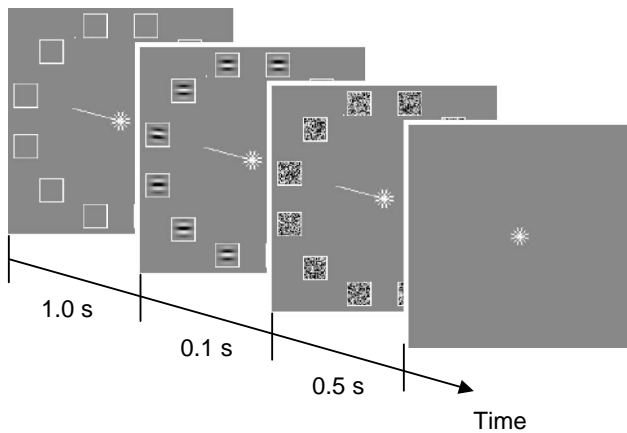


Fig. 1. Diagram of trial sequence in the main experiment. Twelve (or for some observers, eight) Gabor patterns appear for 0.1 s. Twelve (eight) or (as in this case) one limb of a spatial cue precedes the Gabor array by 1 s. A random noise postmask follows it immediately. Observers must report the direction of the target's tilt.

2. Methods

The display (resolution: 512×512 square pixels, 100 Hz; background luminance halfway between the minimum and maximum of 0 and 75 cd/m^2) was programmed in MATLABTM and generated by a Cambridge Research Systems VSGTM 2/3 graphics card. The viewing distance was 0.7 m. MM and CG wore corrective lenses.

Half a second after the observer's response, a set of (1×1 deg) white-outline boxes in the potential target positions was presented for 1 s. On 'cued' trials the boxes were accompanied by a 2-deg line segment connecting the fixation point to the nearest point 2 deg from the centre of the target box. On 'uncued' trials, all positions were precued. After 1 s, the target and distractors (Gabor patterns that were products of Gaussian blobs with space constant $\sigma = 0.1875$ deg centred 4 deg from fixation, and 3-cycle/deg sinusoids with randomised phase) were revealed. After a further 0.1 s, target and distractors were extinguished, and the postmask (in which the luminance of each pixel within each of the boxes was randomly determined from a uniform distribution) was revealed. After a further 0.5 s, the postmask was extinguished, and the observer was required to identify the direction of the target's tilt (CW or ACW) by pressing the corresponding button. Correct responses were indicated with a tone. (All responses to untilted targets were considered correct.)

Each block of 140 trials contained 10 cued trials and 10 uncued trials with targets (in random positions) having each of seven tilts: $-3n$, $-2n$, $-n$, 0 , n , $2n$, $3n$; where the minimum tilt n , necessary to produce smooth psychometric functions, was determined by a brief, informal, preliminary experiment. These psychometric functions (see Fig. 2 for an example) were maximum-likelihood fit with a two-parameter (μ and σ) cumulative Gaussian distribution, where σ was understood to be the threshold tilt for orientation identification. μ reflects the response bias, it is the target tilt that is seen as clockwise and anticlockwise with equal frequency.

3. Results

To verify the absence of crowding, observer performances in two conditions needed to be identical; one in which distracters were absent and another in which distracters were present, but the target position was cued, one second prior to the display onset. Fig. 2A confirms that

crowding was absent for MM (P value:¹ 0.58), but similar confirmation could not be obtained for the naïve observers. Consequently, these observers were asked to try again with eight positions (i.e., one target and either zero or seven distracters), equally spaced along the same iso-eccentric circle, on which 12 stimuli were displayed to MM (as in Fig. 1). With eight positions, AJ's performances (Fig. 2B), were similar in the two conditions (P value: 0.60), but CG's still showed some evidence of crowding (P value: 4.5×10^{-5}): despite the precue, distracters still had an adverse effect on her performance. This can be seen by comparing the slopes of the two (psychometric) functions in Fig. 2C. Thus, the distracters have elevated the threshold tilt. Nonetheless, CG was allowed to complete the main experiment, in which we looked for practice effects on postmasked searches. Here it should be noted that we intentionally refrained from placing any targets or distracters on the horizontal and vertical meridians, on the basis of previous research, which has established that targets directly above fixation are particularly difficult to identify, whether cued or not (Carrasco et al., 2001).

Results of the main experiment (illustrated in Fig. 1) are shown in Fig. 3. Panels A–C show the evolution of tilt thresholds for cued and uncued targets in a sequence of 140-trial blocks. These curves are all pretty flat. Notable exceptions are MM's uncued curve, which does seem to have a gradient just less than zero and both of CG's curves, which drop after the second block of trials. For all observers, the log ratio between uncued and cued thresholds (i.e., the vertical interval between the curves) exceeded that predicted by the max rule (vertical gray lines), throughout the duration of the experiment. Thus, we can be confident² that large cueing effects, the hallmark of attentional capacity limits (Palmer et al., 2000), survive even considerable practice.

Most models of search (see Appendix A) assume that the visual system noisily encodes each distracter and target along the relevant perceptual dimension; in this case, tilt. Therefore, within the framework of any search model, an attentional capacity limit could manifest as increased noise. To investigate the spatial distribution of the performance-limiting noise, we estimated threshold as a function of target position, twice, for each observer; once for the early blocks (Figs. 3D–F), and again for the more recent blocks (panels G–I). Of the three observers, only MM's

¹ These P values are defined as $1 - \chi^2_2(2\ln A)$, where A is the ratio between the maximum likelihood that the data from the two conditions were generated by the same (Gaussian) psychometric function (see Section 2) and the maximum likelihood that they were generated by two psychometric functions having different threshold and bias parameters and χ^2_2 is the cumulative distribution function of a χ^2 random variable with 2 degrees of freedom.

² Measurement error would cause exactly half the ratios to exceed any theoretical value. Since all 12 ratios for MM, 10 ratios for CG, and 8 ratios for AJ are greater than that predicted by the max rule, a comparison with the binomial distribution suggests that, for each observer, we can be more than 95% certain the actual ratio exceeds that predicted by the max rule.

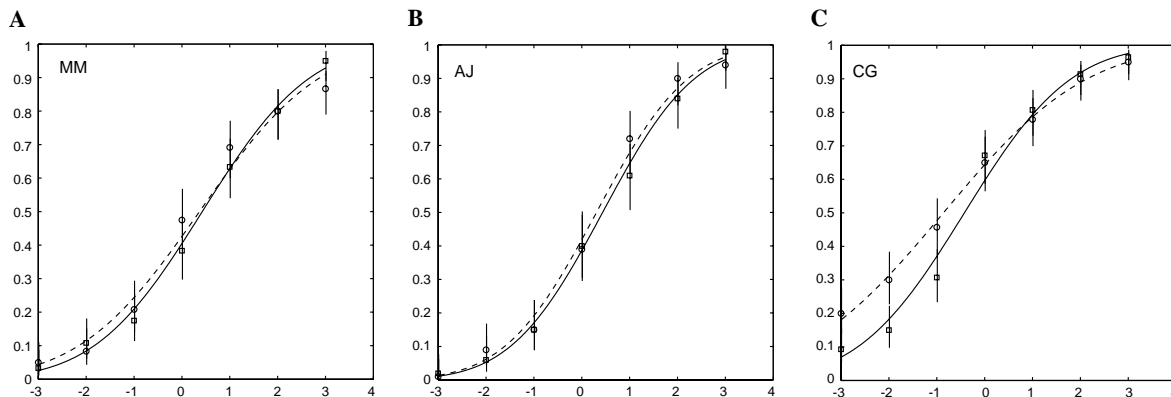


Fig. 2. Effect of distracters on cued targets. A comparison of psychometric functions (two-parameter Gaussians) fit to data obtained with and without distracters (circles/broken line and boxes/solid line, respectively), reveals no effect for MM (A; 11 distracters) or AJ (B; 7 distracters), but a small effect (i.e., ‘crowding’) for CG (C; 7 distracters).

performances were significantly different in these two epochs (P values³ were AJ: 0.19, CG: 0.74, MM: 0.02).

Before proceeding, it must be noted that the spatial distribution of performance-limiting noise cannot be inferred from these thresholds without knowing how an observer combines information from each position when selecting a response. This issue will be addressed below. First, consider the shapes of these plots. They certainly are not very circular (i.e., they are anisotropic). In general, the uncued curves in particular appear to be elongated vertically (Carrasco et al., 2001), indicating that performance was particularly poor when uncued targets appeared near the top and/or bottom of the display. Idiosyncrasies also emerged. CG and, to some extent, AJ’s performances were worst when uncued targets appeared near 11:00 on a virtual clockface. MM performed worst when the target appeared near 5:00 o’clock. Idiosyncrasies such as this would be have been lost, had data been pooled across a large number of observers as in previous studies (Carrasco et al., 2001). Of the cued performances, only MM’s were significantly anisotropic (P values⁴ were AJ: 0.51, CG: 0.10, MM: 0.0003); but *all* uncued performances were significantly anisotropic (P values were all less than 0.001).

4. Discussion

Now let us consider the implications of this anisotropy for observer decision strategies. When adopting the Max Rule,

³ These P values are defined as $1 - \chi^2_{2N} (2 \ln A)$, where N is the number of possible target positions, A is the ratio between the maximum likelihood that the data from the two epochs were generated by the same N (Gaussian) psychometric functions (see Section 2) and the maximum likelihood that they were generated by $(2N)$ psychometric functions having different threshold parameters and χ^2_{2N} is the cumulative distribution function of a χ^2 random variable with $2N$ degrees of freedom.

⁴ These P values are defined as $1 - \chi^2_{N-1} (2 \ln A)$. In this case, A is the ratio between the maximum likelihood that the all the data were generated by the same psychometric function, regardless of target position, and the maximum likelihood that they were generated by N psychometric functions—one for each target position—having different threshold parameters (but identical bias parameters).

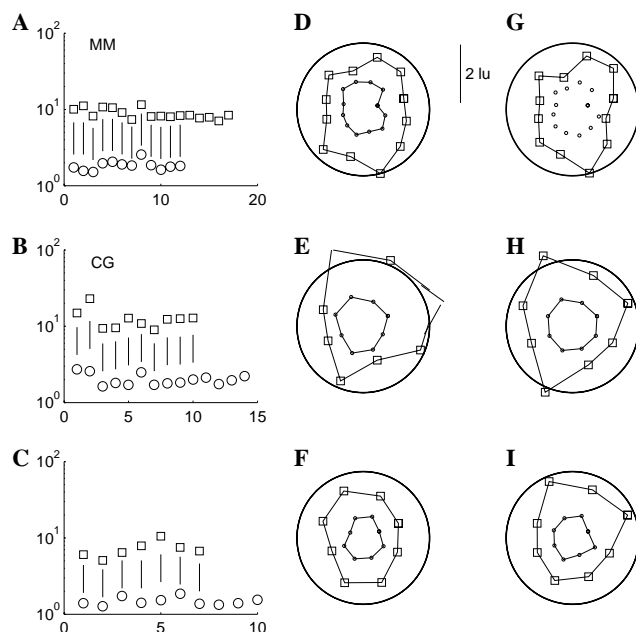


Fig. 3. Results of the main experiment. (A–C) Tilt thresholds as a function of target position in the early (D–F) and late blocks (G–I). A comparison between these epochs reveals stable, idiosyncratic positional effects. Only very large tilts can be correctly identified when the target appears in certain ‘neglected’ positions. Note that the scale in the polar plots is logarithmic (base 10) and that 0.5 log units have been added to every point to prevent negative numbers. Off-scale thresholds for CG are in excess of 200 deg.

most incorrect identification responses will stem from the most noisily encoded position, i.e., where perceived tilt has the greatest variance. Therefore target position should not matter greatly. Increasing the noise at any one position will result in similar elevations of threshold for all targets. Indeed, were the noise effectively zeroed in all but one position, the Max Rule would predict that threshold should become completely independent of target position (proof in Appendix B). Thus, we can be certain that our observers did not use the Max Rule.

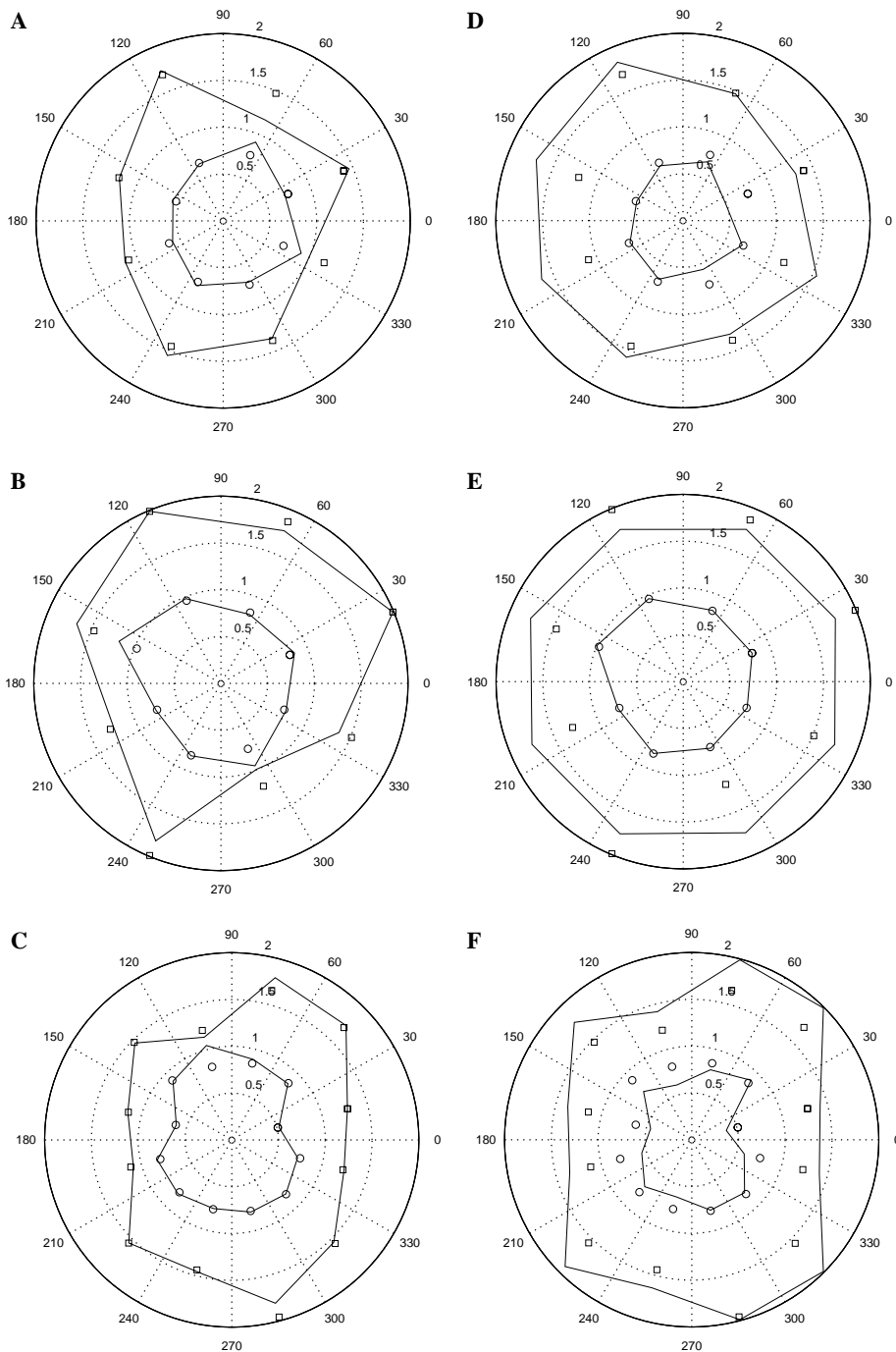


Fig. 4. Fits of Weighted Averaging and Weighted Max models. The circles and boxes reflect cued and uncued thresholds, respectively, a theoretically estimated from psychometric data. Curves reflect maximum-likelihood fits to those same (raw) psychometric data. The Weighted Averaging model (D–F), which overestimates two observers' uncued thresholds but adequately reflects their anisotropy, has $2N - 1$ free parameters, where N is the number of possible target positions. The Weighted Max model (A–C) also has $2N - 1$ free parameters. The polar plots follow the conventions of Fig. 3.

One reason for not adopting the Max Rule is that it is not ideal (Solomon & Morgan, 2001).⁵ The ideal observer

⁵ For comparison, assume the orientation of each Gabor is perturbed by zero-mean Gaussian noise with a variance of 1 deg. According to the Max Rule, threshold with 11 distractors should be 2.45 deg, i.e., a 2.45-deg target will be identified with 84% accuracy. However, the ideal observer would correctly identify a 2.45-deg tilt with 87% accuracy. From this we can infer its uncued threshold should be about 2.17 deg; 11% lower.

selects the most likely orientation (clockwise or anticlockwise), given all possible events. When there is little noise at the target position, performance should be excellent, regardless how much noise is added to each distractor. In particular, if position A had twice as much noise as position B, then the ideal decision rule predicts that the threshold for an uncued target in position A should be more than twice the threshold for an uncued target in position B. Thus, our results appear to be at least qualitatively consis-

tent with an ideal decision rule and inhomogeneously increased noise. On the other hand, without a concomitant increase in noise, set-size effects are too large to be consistent with an ideal decision rule.

Limited computational power precludes finding the position-specific noise-increases that best fit our results, given an ideal decision rule. However, there are simpler models that can be fit. One such model that has been suggested as an alternative to increased noise is tilt averaging, in which responses are based on the mean perceived tilt (Parkes et al., 2001). (Tilt averaging is opposite the Max Rule on the continuum of pooling models described by Minkowski summation.) Of course, thresholds based on true averages must be isotropic, but thresholds based on weighted averages need not. Best fits of a weighted averaging model (e.g., Kinchla, Chen, & Evert, 1995) are shown in Fig. 4 (panels D–F; details in the Appendix A). These fits reflect the anisotropy of actual thresholds very well, but—for MM and AJ, who showed no evidence of crowding—the fits also largely over-estimate the set-size effect; i.e., most predictions are too high. For CG, who did show evidence of crowding in Fig. 2, the fit is excellent. It may be that (weighted) averaging is a better model for identification in the context of crowding (Parkes et al., 2001), rather than in the more general context of visual search. Note that none of the fits could be improved by the addition of late noise to the decision process (Baldassi & Burr, 2000; Parkes et al., 2001). Illustrative fits of the weighted averaging model to full psychometric functions are shown for observer AJ in Fig. 5.

For completeness, we also consider a weighted max model, in which anisotropic weighing of orientation estimates is followed by the Max Rule, instead of averaging.

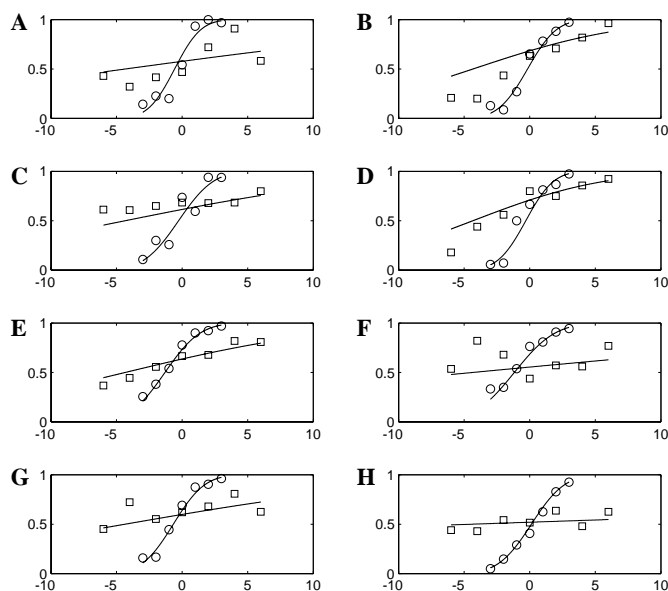


Fig. 5. Illustrative fits of the weighted averaging model to AJ's psychometric functions. (A) Shows the data from the 330 deg position (see Fig. 4) and (B–H) are for the remaining positions, reading anti-clockwise. Circles are for cued and rectangles for the uncued condition.

Best fits of this weighted max model (details in Appendix A) are shown in Fig. 4A–C. Like the weighted averaging fits, these reflect the anisotropy of actual thresholds. For AJ and CG, fits of the weighted averaging model were better than those of the weighted max model. The differences in log likelihoods for the two models were -32 , 20 , and 30 for MM, CG, and AJ, respectively. Because neither model is a nested version of the other there is no straightforward way of attaching significance values to these differences, but differences of greater than 3 are generally thought to be worth taking seriously.

For MM, the fit of the weighted max model was better. We point out that this observer was required to monitor 12 positions, whereas the other two observers were required to monitor just 8. Elsewhere (Solomon & Morgan, 2001) we have shown that, with just two positions, averaging and the max rule both produce ideal behaviour. As the number of positions increases, the max rule becomes less efficient, but averaging becomes less efficient even faster (Baldassi & Verghese, 2002). Thus one could argue that with 12 positions MM had even more incentive to reject a strategy based on averaging.

Finally, it seems that if an observer were compelled to adopt a strategy of weighing orientation estimates prior to averaging or using a Max Rule, the most sensible weights would be those that minimized contributions from positions having high variance. This prediction could have been confirmed by a regression analysis, but in fact proved significant ($P < 0.03$) for MM alone.

All observers (including author MM) were considerably surprised by the anisotropy of their thresholds when they came to know of them. None reported a conscious decision to ignore certain positions or concentrate on others. In a way, their behaviour (with brief, postmasked displays) parallels that of a patient with unilateral neglect: as in neglect, certain positions appear to be ignored only when distracting stimuli appear elsewhere (Driver & Vuilleumier, 2004; Driver, Vuilleumier, & Husan, 2003).

Patients with parietal lesions can overcome their neglect in some cases. To see if this would be true here, MM ran the experiment again, attempting to concentrate on his previously neglected position near 5:00 o'clock. Fig. 6 shows that the effort was only partially successful. Improvement in the lower right visual field was obtained at a cost to the lower left. The overall performance averaged over positions remained the same (Fig. 5 right-hand half); thresholds derived from the psychometric functions changed insignificantly from 8.50 to 8.46 deg. The anisotropy remained highly significant ($P < .001$).

We conclude that visual search for a briefly presented, postmasked, tilted target is capacity limited, in the sense that performance is much worse than predicted by the simple Max Rule. Capacity limitations apparently make it impossible for observers to monitor all the potential targets efficiently, and they react by virtually neglecting certain positions at the expense of others. The positions that are neglected are only partly predictable from the noise that is measured in the cued condition. The correlations (Ken-

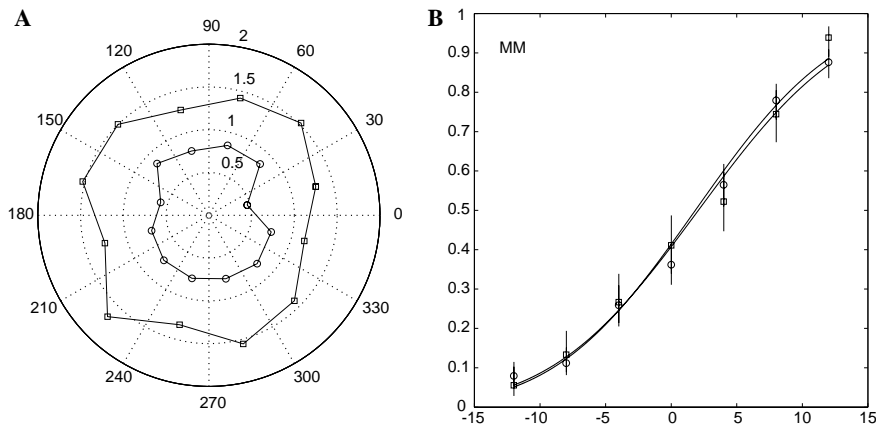


Fig. 6. MM's attempt to overcome his neglect. A comparison of the left-hand side of the figure with the comparable plot in Fig. 4 shows that improvement at the 5:00 o'clock position was balanced by decrements in other positions. The right-hand half shows that the overall psychometric functions before (circles) and after (boxes) the attempt to overcome neglect remained the same.

dall's τ) between uncued and cued thresholds (see Fig. 2) were positive but modest. Moreover, the pattern of neglect could be shifted to some extent by attending to previously neglected positions (Fig. 5). Given that some positions have to be neglected, the observer apparently reacts ideally by giving little weight to these positions. We suggest that this apparently unconscious weighting of attention in normal observers may serve as a useful model for the clinical condition of neglect.

Acknowledgment

This study was supported by a Grant from the EPSRC.

Appendix A

In our analyses, the simple and weighted Max Rules, the ideal observer and weighted averaging all adhere to Signal-Detection Theory (Green & Swets, 1966), in which the orientation of each Gabor is encoded independently, with additive Gaussian noise. For simplicity, we adopt the following notation for normal density (PDF) and distribution (CDF):

$$f(x; \mu, \sigma) = \frac{1}{\sqrt{2\pi\sigma}} e^{-\frac{(x-\mu)^2}{2\sigma^2}} \quad (1)$$

and

$$F(x; \mu, \sigma) = \int_{-\infty}^x du f(u; \mu, \sigma). \quad (2)$$

In our models, when a Gabor in position i has tilt θ , the density and distribution of its apparent tilt can be abbreviated as

$$f_{\theta,i}(x) = f(x; \theta + \mu_i, \sigma_i) \quad (3)$$

and

$$F_{\theta,i}(x) = F(x; \theta + \mu_i, \sigma_i). \quad (4)$$

For an unbiased observer, the average apparent tilt would equal the actual tilt (i.e., $\mu_i = 0$). For the biased observer, the sensory bias μ_i , is indistinguishable from a physical tilt. All of our model observers were unbiased.

Let $E_{\theta,i}$ denote the generic event that a target appears in position i , with (anticlockwise) tilt $\theta > 0$.⁶ Let X_i describe the target's apparent tilt and $X_j, j \neq i$ describe a distracter's apparent tilt. If $X_i = x$, the target will have a larger apparent tilt (clockwise or anticlockwise) than any of the distracters when $|X_j| < x, \forall j \neq i$. When all apparent tilts are independent, this will happen with probability $\prod_{j \neq i} P(|X_j| < x) = \prod_{j \neq i} [F_{0,j}(x) - F_{0,j}(-x)]$. Thus, $\int_0^\infty dx f_{\theta,i}(x) \prod_{j \neq i} [F_{0,j}(x) - F_{0,j}(-x)]$ is the probability that the target produces a larger (anticlockwise) apparent tilt than any of the distracters and $\int_0^\infty dx f_{0,j}(x) [F_{\theta,i}(x) - F_{\theta,i}(-x)] \prod_{k \neq i,j} [F_{0,k}(x) - F_{0,k}(-x)]$ is the probability that a distracter in position j produces a larger (anticlockwise) apparent tilt than the target (still in position i) or any of the other distracters. Thus, according to the simple Max Rule, the probability of a correct identification I , is

$$P_{\text{Max}}(I|E_{\theta,i}) = \int_0^\infty dx f_{\theta,i}(x) \prod_{j \neq i} [F_{0,j}(x) - F_{0,j}(-x)] + \sum_{j \neq i} \int_0^\infty dx f_{0,j}(x) [F_{\theta,i}(x) - F_{\theta,i}(-x)] \times \prod_{k \neq i,j} [F_{0,k}(x) - F_{0,k}(-x)]. \quad (5)$$

For the Weighted Max Rule, an arbitrary weight a_i can be assigned to the apparent tilt in each position. Thus, the probability of a correct identification becomes

⁶ For any unbiased observer, the probability of correctly identifying a clockwise target is identical to the probability of correctly identifying an anticlockwise target. Thus, we need only consider the latter.

$$\begin{aligned}
 P_{\text{WtMax}}(I|E_{\theta,i}) &= \int_0^\infty dx f_{a_i\theta,a_i}(x) \prod_{j \neq i} [F_{0,a_j}(x) \\
 &\quad - F_{0,a_j}(-x)] + \sum_{j \neq i} \int_0^\infty dx f_{0,a_j}(x) \\
 &\quad \times [F_{a_i\theta,a_i}(x) - F_{a_i\theta,a_i}(-x)] \\
 &\quad \times \prod_{k \neq i,j} [F_{0,a_k}(x) - F_{0,a_k}(-x)]. \quad (6)
 \end{aligned}$$

The ideal observer selects the most likely orientation (clockwise or anticlockwise), given all possible events. In order to compute its accuracy $P_{\text{Ideal}}(I|E_{\theta,i})$, we need to determine how many of the possible sensations are more likely under the null hypothesis $H_0: \theta > 0$ than under the alternative $H_1: \theta < 0$ [NB: $P_{\text{Ideal}}(I|E_{0,i}) = 1/2 \forall i$].

In particular, let $\cup_{x>0} E_{x,\cdot}$ and $\cup_{x<0} E_{x,\cdot}$ denote all possible events given an anticlockwise and clockwise target, respectively. Let the vector $\mathbf{x} = [x_1 \ x_2 \ \dots \ x_N]$ represent the sensations arising from each position on a given trial. Thus,

$$\begin{aligned}
 P_{\text{Ideal}}(I|E_{\theta,i}) &= \int_{-\infty}^\infty dx_N \dots \int_{-\infty}^\infty dx_1 P(\mathbf{x}|E_{\theta,i}) \\
 &\quad \times H[P(\mathbf{x}|\cup_{x>0} E_{x,\cdot}) - P(\mathbf{x}|\cup_{x<0} E_{x,\cdot})] \\
 &= \int_{-\infty}^\infty dx_N \dots \int_{-\infty}^\infty dx_1 P(\mathbf{x}|E_{\theta,i}) \\
 &\quad \times H\left(\sum_j \left[\sum_{x>0} P(\mathbf{x}|E_{x,j}) - \sum_{x<0} P(\mathbf{x}|E_{x,j})\right]\right), \quad (7)
 \end{aligned}$$

where $H(x)$ is the (Heaviside) unit-step function:

$$H(x) = \begin{cases} 1 & x > 0, \\ 1/2 & x = 0, \\ 0 & x < 0. \end{cases} \quad (8)$$

Therefore

$$\begin{aligned}
 P_{\text{Ideal}}(I|E_{\theta,i}) &= \int_{-\infty}^\infty dx_N \dots \int_{-\infty}^\infty dx_1 f_{\theta,i}(x_i) \prod_{k \neq i} f_{0,k}(x_k) \\
 &\quad \times H\left[\sum_j \prod_{l \neq j} f_{0,l}(x_l) \sum_{x>0} f_{x,j}(x_j) - f_{-x,j}(x_j)\right]. \quad (9)
 \end{aligned}$$

Finally, an observer who, prior to averaging, applies a weight of a_i to the apparent tilt in position i , will respond with accuracy

$$P_{\text{Avg}}(I|E_{\theta,i}) = F_{0,1}\left(\frac{a_i\theta}{\sqrt{\sigma_i^2 + \sum_j a_j\sigma_j^2}}\right), \quad (10)$$

where σ_i^2 denotes the variance of the late Gaussian noise.

Appendix B

Here, we prove that if the noise were effectively zeroed in all but one position, the Max Rule would predict that

threshold should become completely independent of target position. Following the notation introduced in Appendix A, let $\sigma_j = 0 \forall j \neq 1$. This effectively zeroes the noise in all but the first position. Consequently,

$$f_{\theta,j}(x) = \delta(x - \theta) \quad (11)$$

and

$$F_{\theta,j}(x) = H(x - \theta) \quad (12)$$

for all $j \neq 1$. NB: the delta function $\delta(x - \theta)$ is the derivative of the unit step. Now consider the probability of a correct identification in the event that the target appears at the noisy position. From Eq. (5) we have

$$\begin{aligned}
 P_{\text{Max}}(I|E_{\theta,1}) &= \int_0^\infty dx f_{\theta,1}(x) \prod_{j \neq 1} [F_{0,j}(x) - F_{0,j}(-x)] \\
 &\quad + \sum_{j \neq 1} \int_0^\infty dx f_{0,j}(x) [F_{\theta,1}(x) \\
 &\quad - F_{\theta,1}(-x)] \prod_{k \neq i,1} [F_{0,k}(x) - F_{0,k}(-x)]. \quad (13)
 \end{aligned}$$

Substituting (11) and (12) into (13) we have

$$\begin{aligned}
 P_{\text{Max}}(I|E_{\theta,1}) &= \int_0^\infty dx f_{\theta,1}(x) \prod_{j \neq 1} [H(x) - H(-x)] \\
 &\quad + \sum_{j \neq 1} \int_0^\infty dx \delta(x) [F_{\theta,1}(x) - F_{\theta,1}(-x)] \\
 &\quad \times \prod_{k \neq i,1} [H(x) - H(-x)]. \quad (14)
 \end{aligned}$$

However, $\delta(x)[H(x) - H(-x)] = 0 \forall x$, thus (14) can be greatly simplified to:

$$P_{\text{Max}}(I|E_{\theta,1}) = \int_0^\infty dx f_{\theta,1}(x). \quad (15)$$

Finally, this can be expressed as a function of the standard normal c.d.f.

$$P_{\text{Max}}(I|E_{\theta,1}) = 1 - \Phi(-\theta/\sigma_1). \quad (16)$$

Now consider the probability of a correct identification in the event that the target appears at another position. Again, from Eq. (5) we have

$$\begin{aligned}
 P_{\text{Max}}(I|E_{\theta,j}) &= \int_0^\infty dx f_{\theta,j}(x) [F_{0,1}(x) - F_{0,1}(-x)] \\
 &\quad \times \prod_{i \neq j,1} [F_{0,i}(x) - F_{0,i}(-x)] \\
 &\quad + \int_0^\infty dx f_{0,1}(x) [F_{\theta,j}(x) - F_{\theta,j}(-x)] \\
 &\quad \times \prod_{k \neq j,1} [F_{0,k}(x) - F_{0,k}(-x)] \\
 &\quad + \sum_{i \neq j,1} \int_0^\infty dx f_{0,i}(x) [F_{\theta,j}(x) - F_{\theta,j}(-x)] \\
 &\quad \times [F_{0,1}(x) - F_{0,1}(-x)] \prod_{k \neq j,1,i} [F_{0,k}(x) - F_{0,k}(-x)]. \quad (17)
 \end{aligned}$$

Substituting (11) and (12) into expression (17), we have

$$\begin{aligned}
P_{\text{Max}}(I|E_{\theta,j}) &= \int_0^{\infty} dx \delta(x - \theta) [F_{0,1}(x) - F_{0,1}(-x)] \\
&\times \prod_{i \neq j, 1} [H(x) - H(-x)] \\
&+ \int_0^{\infty} dx f_{0,1}(x) [H(x - \theta) - H(-x - \theta)] \\
&\times \prod_{k \neq j, 1} [H(x) - H(-x)] \\
&+ \sum_{i \neq j, 1} \int_0^{\infty} dx \delta(x) [H(x - \theta) - H(-x - \theta)] \\
&\times [F_{0,1}(x) - F_{0,1}(-x)] \prod_{k \neq j, 1, i} [H(x) - H(-x)].
\end{aligned} \tag{18}$$

Again, since $\delta(x)[H(x) - H(-x)] = 0 \forall x$, the last term of (18) disappears and the first two can be greatly simplified to:

$$\begin{aligned}
P_{\text{Max}}(I|E_{\theta,j}) &= F_{0,1}(\theta) - F_{0,1}(-\theta) + \int_0^{\infty} dx f_{0,1}(x) \\
&= F_{0,1}(\theta) - F_{0,1}(-\theta) + 1 - F_{0,1}(\theta) \\
&= 1 - F_{0,1}(-\theta) \\
&= 1 - \Phi(-\theta/\sigma_1) \\
&= P_{\text{Max}}(I|E_{\theta,1}).
\end{aligned} \tag{19}$$

Q.E.D.

References

- Baldassi, S., & Burr, D. C. (2000). Feature-based integration of orientation signals in visual search. *Vision Research*, *40*, 1293–1300.
- Baldassi, S., & Verghese, P. (2002). Comparing integration rules in visual search. *Journal of Vision*, *2*, 559–570. <<http://journalofvision.org/2/8/3/>>.
- Carrasco, M., Talgar, C. P., & Cameron, E. L. (2001). Characterising visual performance fields: effects of transient covert attention, spatial frequency, eccentricity, task and set size. *Spatial Vision*, *15*, 61–75.
- Driver, J., & Vuilleumier, P. (2004). *Spatial neglect*, *Encyclopedia of Cognitive Science*. New York: Macmillan.
- Driver, J., Vuilleumier, P., & Husan, M. (2003). Spatial neglect and extinction. In M. Gazzaniga (Ed.), *The new cognitive neurosciences*. Cambridge: MIT Press.
- Green, D. M., & Swets, J. A. (1966). *Signal Detection Theory and Psychophysics* (1st ed.). New York: Wiley.
- Kinchla, R. A., Chen, Z., & Evert, D. (1995). Precue effects in visual search: Data or resource limited? *Perception & Psychophysics*, *57*(4), 441–450.
- Morgan, M., Castet, E., & Ward, R. (1998). Visual search for a tilted target: Tests of the spatial uncertainty model. *Quarterly Journal of Experimental Psychology*, *51*, 347–371.
- Morgan, M. J., & Solomon, J. A. (2005). Capacity limits for spatial discrimination. In L. Itti, G. Rees, & J. Tsotsos (Eds.), *Neurobiology of attention*. Elsevier.
- Palmer, J. (1994). Set-Size effects in visual search: The effect of attention is independent of the stimulus for simple tasks. *Vision Research*, *32*, 1703–1721.
- Palmer, J., Verghese, P., & Pavel, M. (2000). The psychophysics of visual search. *Vision Research*, *40*(10–12), 1227–1268.
- Parkes, L., Lund, J., Angelucci, A., Solomon, J. A., & Morgan, M. (2001). Compulsory averaging of crowded orientation signals in human vision. *Nature Neuroscience*, *4*(7), 739–744.
- Solomon, J. A., & Morgan, M. J. (2001). Odd-men-out are poorly localized in brief displays. *Investigative Ophthalmology Visual Science*, *42*(4), 4973.